

## Electronic Supplementary Information

### Theoretical capacity achieved in a $\text{LiMn}_{0.5}\text{Fe}_{0.4}\text{Mg}_{0.1}\text{BO}_3$ cathode by using topological disorder

Jae Chul Kim, Dong-Hwa Seo, and Gerbrand Ceder\*

Department of Materials Science and Engineering, Massachusetts Institute of Technology, Cambridge, MA 02139, USA

Corresponding author's email: gceder@mit.edu

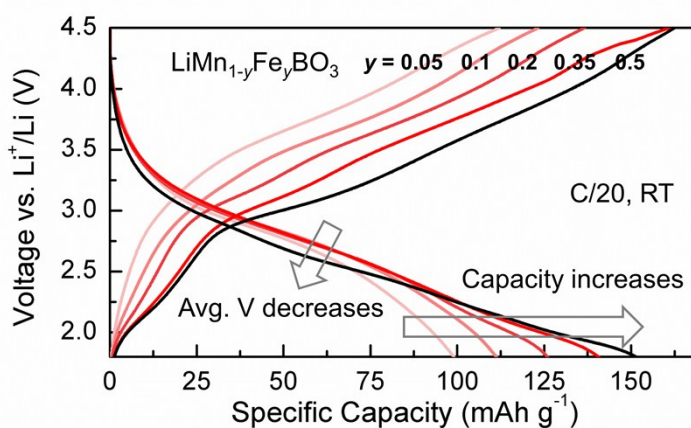


**Figure S1.** Voltage vs. capacity profiles for  $\text{LiMn}_{1-y}\text{Fe}_y\text{BO}_3$  for a C/20 rate at RT. As the amount of Fe substitution increases, the specific capacity accordingly increases, but average voltage decreases.

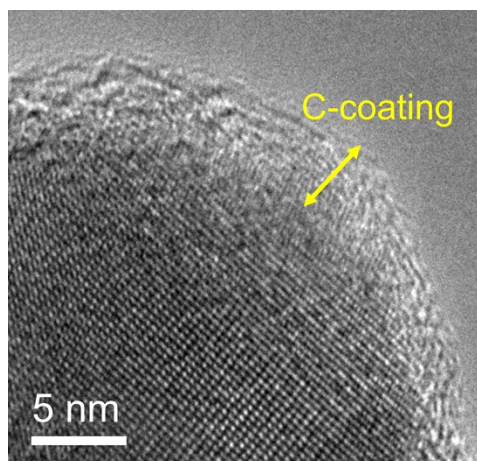


**Figure S2.** HRTEM image of the carbon coated  $\text{LiMn}_{0.5}\text{Fe}_{0.4}\text{Mg}_{0.1}\text{BO}_3$  particle. The coating is 3~4 nm thick.

### Ab initio computation

The mixing state for two or more compounds can be estimated from the enthalpy of mixing ( $\Delta H_{\text{mix}}$ ), which is, by definition, the enthalpy ( $H = E + pdV$ ) difference between a mixture product and individual reactants. Thus, the sign of  $\Delta H_{\text{mix}}$  can thermodynamically specify whether the mixture will form a solid solution (small  $\Delta H_{\text{mix}}$ ), undergo phase separation (large positive  $\Delta H_{\text{mix}}$ ), or result in cation ordering (large negative  $\Delta H_{\text{mix}}$ ). For a reaction between solids,  $\Delta H_{\text{mix}}$  is often approximated by the (internal) energy of mixing ( $\Delta E_{\text{mix}}$ ) since the  $pdV$  term is rather insignificant. Therefore, the mixing state for  $\text{LiMn}_{1-y-z}\text{Fe}_y\text{Mg}_z\text{BO}_3$  can be determined, as specified in Equation S1.

$$\Delta E_{\text{mix}} = E(\text{LiMn}_{1-y-z}\text{Fe}_y\text{Mg}_z\text{BO}_3) - [(1 - y - z) \times E(\text{LiMnBO}_3) + y \times E(\text{LiFeBO}_3) + z \times E(\text{LiMgBO}_3)] \quad (\text{S1})$$

where

$y = 0.375$  and  $z = 0.125$ ,

$E(\text{LiMnBO}_3) = -43.813$ ,  $E(\text{LiFeBO}_3) = -41.782$ , and  $E(\text{LiMgBO}_3) = -40.200$  eV per formula unit.

The energies of 100 symmetrically distinct  $\text{LiMn}_{0.5}\text{Fe}_{0.375}\text{Mg}_{0.125}\text{BO}_3$  configurations were obtained by *ab initio* computation and are plotted in Figure S3. By taking the energy of the most stable configuration, the calculated energy of mixing ( $\Delta E_{\text{mix}}$ ) of  $\text{LiMn}_{0.5}\text{Fe}_{0.375}\text{Mg}_{0.125}\text{BO}_3$  is 1.5 meV per formula unit, which can be obtained from Equation S1. While the formation energy is positive, it is very small, suggesting that at elevated temperatures, entropy of mixing will overcome the positive  $\Delta H_{\text{mix}}$  and result in solid solution.

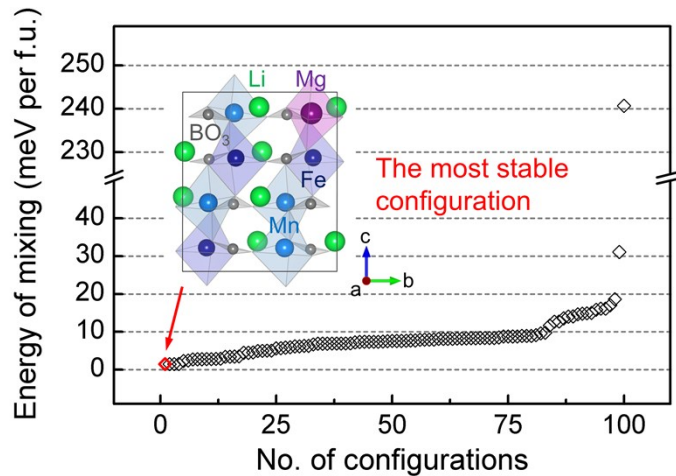


**Figure S3.** Calculated formation energies of 100 distinct  $\text{LiMn}_{0.5}\text{Fe}_{0.375}\text{Mg}_{0.125}\text{BO}_3$  configurations. The lowest energy of mixing is 1.5 meV, leading to formation of solid solution at elevated temperature due to the entropic effect.

**Table S1.** Ground state phases of  $\text{Li}_{1-x}\text{Mn}_{0.5}\text{Fe}_{0.375}\text{Mg}_{0.125}\text{BO}_3$  with respect to a Li content,  $x$ 

$x$	$\text{Li}_{1-x}\text{Mn}_{0.5}\text{Fe}_{0.375}\text{Mg}_{0.125}\text{BO}_3$	
	$\Delta E$ (meV)	Ground states
0	1.5	$\text{LiMnBO}_3$ , $\text{LiFeBO}_3$ , and $\text{LiMgBO}_3$
0.375	48.6	$\text{LiBO}_2$ , $\text{Li}_2\text{B}_4\text{O}_7$ , $\text{Mg}_2\text{B}_2\text{O}_5$ , $\text{Mn}(\text{FeO}_2)_2$ , and $\text{LiMnBO}_3$
0.625	91.1	$\text{Li}_3\text{B}_7\text{O}_{12}$ , $\text{Fe}_2\text{O}_3$ , $\text{Mg}_2\text{B}_2\text{O}_5$ , $\text{Mn}_3\text{O}_4$ , and $\text{Mn}(\text{FeO}_2)_2$
0.875	113.3	$\text{MgB}_4\text{O}_7$ , $\text{Mn}_2\text{O}_3$ , $\text{MnB}_4\text{O}_7$ , $\text{Fe}_2\text{O}_3$ , $\text{MnO}_2$ , and $\text{Li}_3\text{B}_7\text{O}_{12}$
1	N/A	N/A

**Table S2.** Elemental analysis of Li, Mn, Fe, Mg, and B by the current plasma emission spectroscopy (ASTM E 1097-07).

Elements	Li	Mn	Fe	Mg	B
Ideal atomic %	1	0.5	0.4	0.1	1
Actual atomic %	1.06	0.50	0.41	0.1	1.01

## Rietveld refinement

To perform Rietveld refinement, a reference structure for the solid solution compound was generated by modifying  $\text{LiMnBO}_3$  in the ICSD (No. 200535)<sup>1</sup> to contain 50% Mn, 40% Fe, and 10% Mg. Parameters including scale factor, lattice constants, peak profile parameters, atomic coordinates, site occupancy factors, preferred orientation, and overall temperature factors were refined step-by-step, and each of them was confirmed or rejected to produce the best fitting agreement. Considering the atomic ratio in Table S2, the total amount of each cation was constrained to be stoichiometric, but their site occupancy factors (SOFs) were allowed to vary between two non-equivalent sites in the trigonal bipyramidal polyhedron. We obtain 2% and 9.6% disorder for Li-Mn and Li-Fe pairs, respectively. Li-Mg disorder cannot be refined. However, this does not exclude the possibility of Mg occupancy in the Li site due to the weak scattering power of existing Mg antisite as the diffraction peaks from site disorder reflect a lump sum of all the scattering powers of Mn, Fe, and Mg antisites.

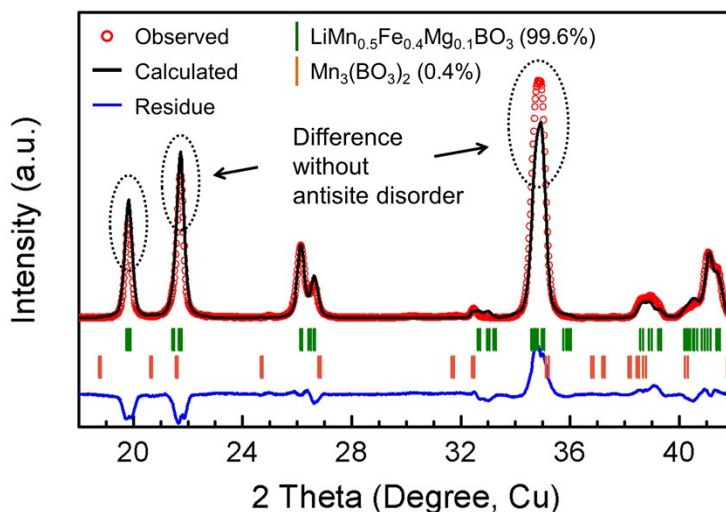


**Figure S4.** Profile matching of XRD pattern obtained from  $\text{LiMn}_{0.5}\text{Fe}_{0.4}\text{Mg}_{0.1}\text{BO}_3$  fired at 550°C, assuming no antisite disorder. The calculated pattern significantly mismatches to the observed pattern.

**Table S3.** The result of Rietveld-refinement for  $\text{LiMn}_{0.5}\text{Fe}_{0.4}\text{Mg}_{0.1}\text{BO}_3$ . The occupancies of Li(1), Li(2), B, O(1), O(2), and O(3) sites are not refined.

---

Space group: C 2/c

Unit cell:  $a = 5.169(9) \text{ \AA}$ ,  $b = 8.899(1) \text{ \AA}$ ,  $c = 10.2277(1) \text{ \AA}$ ,  $\beta = 91.19(3)^\circ$

Volume =  $470.44(9) \text{ \AA}^3$

Radiation  $\lambda = 1.5406 \text{ \AA}$ ,  $15^\circ < 2\theta < 75^\circ$

Scale factor: 0.027679, Preferred orientation: 1.05271, B overall: 3.9477

U = 0.089719, V = -0.006491, W = 0.07359, Pseudo-Voigt fit

$R_{\text{wp}} = 5.56692$ ,  $R_p = 3.61066$

---

Atom	Site	x	y	z	SOF
Li(1)	8f	0.1414(0)	0.0016(9)	0.6565(1)	0.5
Li(2)	8f	0.1672(1)	0.0235(9)	0.1847(4)	0.5
Mn(1)	8f	0.1877(2)	0.3318(8)	0.1269(7)	0.24(0)
Mn(2)	8f	0.1142(2)	0.3489(8)	0.1161(3)	0.24(0)
Fe(1)	8f	0.1973(9)	0.3217(7)	0.1363(5)	0.1114(5)
Fe(2)	8f	0.1470(0)	0.3418(7)	0.1063(3)	0.1924(2)
Mg(1)	8f	-0.2440(1)	0.5136(1)	-0.7563(6)	0.0506(0)
Mg(2)	8f	0.1582(0)	0.3384(0)	0.1173(0)	0.0494(1)
B	8f	0.3329(0)	0.1715(0)	0.3747(0)	1
O(1)	8f	0.3944(8)	0.1522(5)	0.1023(4)	1
O(2)	8f	0.2297(2)	0.3049(0)	0.3428(8)	1
O(3)	8f	0.1710(5)	0.0339(5)	0.3728(4)	1
Mn <sub>Li</sub> (1)	8f	-0.1459(2)	-0.0842(4)	0.5678(6)	0.002(0)
Mn <sub>Li</sub> (2)	8f	0.2885(7)	-0.1459(4)	0.2213(1)	0.018(0)
Fe <sub>Li</sub> (1)	8f	0.4772(5)	0.1823(7)	0.4723(8)	0.0370(6)
Fe <sub>Li</sub> (2)	8f	0.0631(7)	0.03820(4)	0.1250(6)	0.0590(7)

---

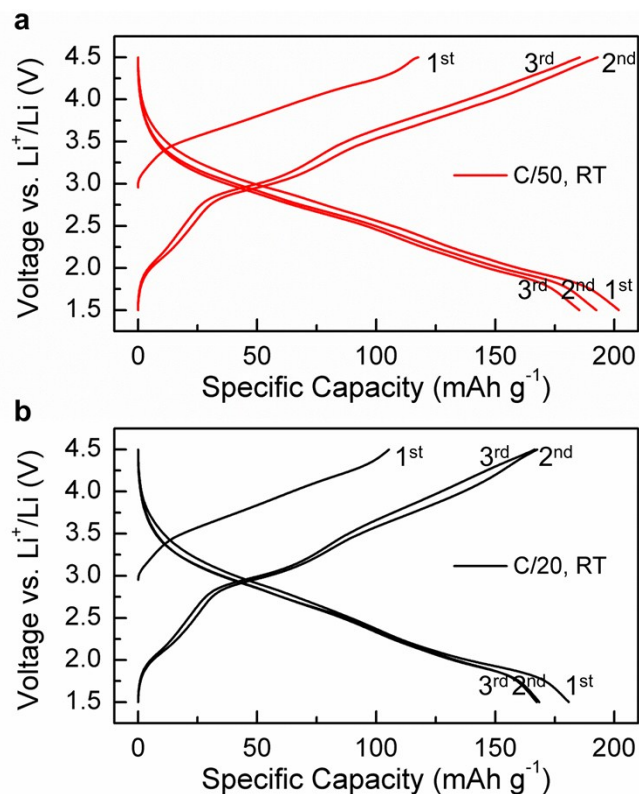


**Figure S5.** Voltage vs. capacity profiles of  $\text{LiMn}_{0.5}\text{Fe}_{0.4}\text{Mg}_{0.1}\text{BO}_3$  at RT. At a C/50 rate, the first discharge capacity is more than  $200 \text{ mAh g}^{-1}$ . At a C/20 rate, the first discharge capacity is  $182 \text{ mAh g}^{-1}$ . In both cases, charge capacities in the first cycle is about  $110 \text{ mAh g}^{-1}$ , which is due to oxidation of  $\text{Fe}^{2+}$  by moisture at surface. This disappears in following cycles.

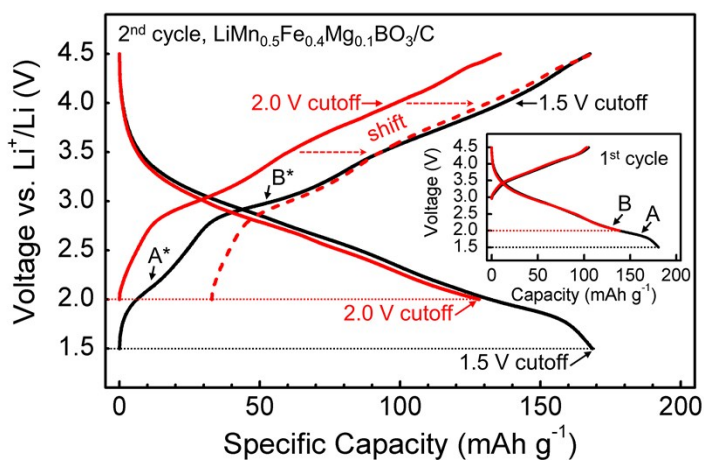


**Figure S6.** Voltage-capacity profiles of  $\text{LiMn}_{0.5}\text{Fe}_{0.4}\text{Mg}_{0.1}\text{BO}_3/\text{C}$  with two different voltage cutoffs (4.5 – 2.0 V and 4.5 – 1.5 V). By comparing the first discharge curves with the different cutoffs in the inset, the capacity obtained between 2.0 and 1.5 V is  $42 \text{ mAh g}^{-1}$ , which is 20.5% of the theoretical capacity. In the second cycle, if the cathode is cycled between 4.5 and 2.0 V, the obtained discharge capacity is  $128 \text{ mAh g}^{-1}$  while  $169 \text{ mAh g}^{-1}$  is achieved with 1.5 V cutoff. Discharging at 2.0 V does not lead to full reduction of  $\text{Fe}^{3+}$  due to inaccessible A and incomplete B reactions, as shown in the inset, where A and B correspond the  $\text{Fe}^{3+}$  reduction in the Li sites and transition metal sites, respectively (asterisks for the corresponding charging reactions).

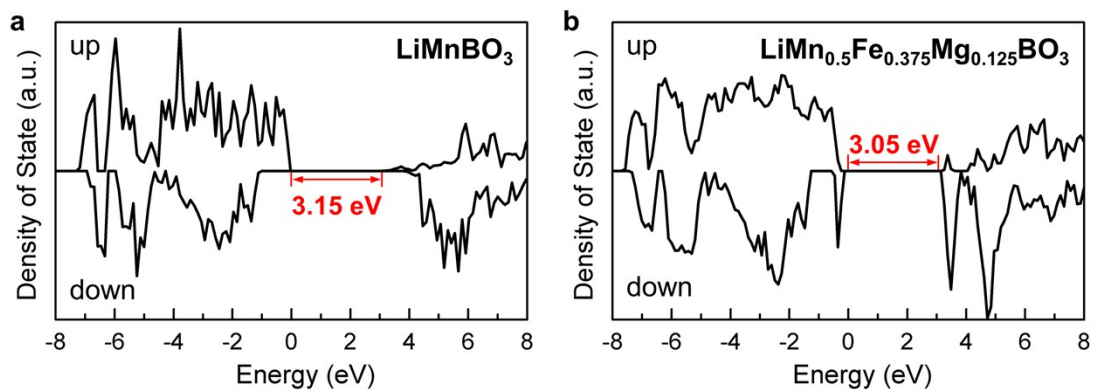


**Figure S7.** Calculated densities of states (DOS) of (a)  $\text{LiMnBO}_3$  and (b)  $\text{LiMn}_{0.5}\text{Fe}_{0.375}\text{Mg}_{0.125}\text{BO}_3$

## References

1. O. S. Bondareva, M. A. Simonov, Y. K. Egorovtismenko and N. V. Belov, *Sov. Phys. Crystallogr.*, 1978, **23**, 269-271.